Scaling Properties of Identified Hadron Production in Au+Au and Cu+Cu Collisions at RHIC-PHENIX

M. Konno[1] (for the PHENIX Collaboration)

(Graduate School of Pure and Applied Sciences, University of Tsukuba, Tsukuba, Ibaraki 305-8571, Japan)

Abstract   Particle type dependences of hadron yield and emission patterns, especially its difference between mesons and baryons, at intermediate p_T (2—5GeV/c) is one of the findings in heavy ion collisions at RHIC. A systematic study of identified hadron production was performed in Au+Au/Cu+Cu collisions at $\sqrt{s_{NN}}$=62.4/200GeV, to investigate the possible origins of this difference. In this paper, we show particle ratios, elliptic flow strengths, and their scaling properties.

Key words   scaling, identified hadron, heavy ion collision

1   Introduction

Studies of identified hadron production in heavy ion collisions at RHIC show particle type dependences of hadron yields, especially a meson/baryon difference at intermediate p_T (2—5GeV/c). In central Au+Au collisions at $\sqrt{s_{NN}} = 200$GeV, there is a significant suppression in meson yields (π, K, etc.) compared to peripheral Au+Au or p+p results. In contrast, a large enhancement of baryons (p, $\overline{p}$, Λ, etc.) relative to mesons is observed at intermediate p_T[1]. On the other hand, in elliptic flow measurements, a meson/baryon difference is also found in its magnitude (v_2 as a function of p_T)[2]. The intermediate p_T region is considered to have both soft and hard hadron production mechanisms. Here, soft part includes hydrodynamic flow[3], quark recombination[4], and hard part includes jet fragmentation and its quenching. The relative magnitudes of these mechanisms are not yet fully understood. A systematic scan over different collision systems (colliding species, beam energies) at RHIC is one of the effective ways to investigate the relative contributions of those production mechanisms. This allows us to study various dependences, such as collision energy, system size, and overlapping geometry, of the hadron production.

2   Data analysis

Data sets used here are Au+Au/Cu+Cu collisions at $\sqrt{s_{NN}} = 62.4/200$GeV taken by PHENIX. Events with a vertex position along the beam axis within $|z| <$30cm were triggered by the Beam-Beam Counters (BBC) located at $|\eta| = 3.0$—3.9. The minimum bias data sample is subdivided into different centrality bins, where a collision centrality is determined from the charged particle multiplicity measured by the BBC.

Charged particle tracks are reconstructed at mid-rapidity $|\eta| <$0.35 using a drift chamber and pad chambers. Particle identification is performed with a time-of-flight ($\sigma_{TOF}\sim$120ps) detector and an aerogel Cherenkov detector ($n \sim$1.011). The aerogel detector was used only for spectra measurements. Corrections to the charged particle spectrum for geometrical acceptance, decay in flight, tracking efficiency are determined using a single-particle GEANT Monte Carlo simulation. Multiplicity-dependent corrections are evaluated by embedding simulated tracks into real

events. No weak decay feed-down correction is applied to the results presented in this paper.

Elliptic flow measurements were done with the reaction plane method for the 200GeV Au+Au/Cu+Cu data. The reaction plane is determined by particle hits in the two BBCs. A large η gap between the central arms and the BBCs reduce the influence of non-flow contributions such as jets.

3   Results

3.1   p/π ratio

Figure 1 shows p/π^+ and $\overline{\mathrm{p}}/\pi^-$ ratios as a function of p_{T} for different centralities in Au+Au collisions at $\sqrt{s_{\mathrm{NN}}} = 200$GeV. The p/$\pi$ ratios in intermediate p_{T} range show a clear centrality dependence with higher relative proton production in more central collisions. A definite turnover is observed for all centrality classes. The peak position is at 2—3GeV/c independent of centrality (STAR also reports similar results[5]). Beyond the peak, the ratios are falling toward the values in p+p collisions, though with the current limited statistics no conclusion can be drawn whether the ratios at high p_{T} in Au+Au are the same as in p+p. The observed behavior indicates a transition from soft to hard hadron production at intermediate p_{T}. Similar p_{T} dependence of p/π is also observed in Cu+Cu collisions at $\sqrt{s_{\mathrm{NN}}} = 200$GeV. Also at 62.4GeV, similar p_{T} dependence is observed in both Au+Au/Cu+Cu collisions. Comparing to the 200GeV data, the 62.4GeV data shows a slightly larger proton contribution at intermediate p_{T}, while there is a less antiproton contribution.
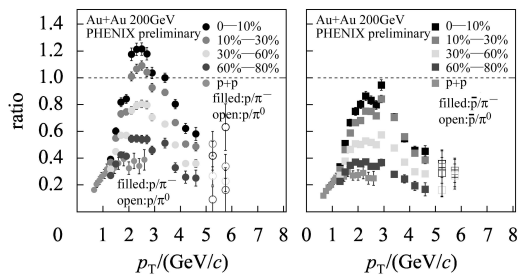

Fig. 1.   p/π^+ (left) and $\overline{\mathrm{p}}/\pi^-$ (right) ratios for different centralities in Au+Au collisions at $\sqrt{s_{\mathrm{NN}}} = 200$GeV.

Figure 2 shows p/π^+ ($\overline{\mathrm{p}}/\pi^-$) ratio as a function of $N_{\mathrm{part}}^{1/3}$ at $p_{\mathrm{T}} = 2$—3GeV/c in Au+Au/Cu+Cu col-

lisions at $\sqrt{s_{\mathrm{NN}}} = 200$GeV. Even though the overlap region of colliding nuclei has a different geometrical shape for the same number of participating nucleons N_{part}, the data shows similar system size ($N_{\mathrm{part}}^{1/3}$) dependences in both systems. This could be called a N_{part} scaling on p/π ratio at the same collision energy. The N_{part} scaling is also observed at lower energy $\sqrt{s_{\mathrm{NN}}} = 62.4$GeV in Au+Au/Cu+Cu.
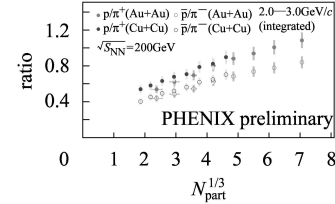

Fig. 2.   p/π ratio as a function of $N_{\mathrm{part}}^{1/3}$ for 2—3GeV/c in Au+Au/Cu+Cu at 200GeV.

On the other hand, the N_{part} scaling is not observed between 62.4GeV and 200GeV in Au+Au. Instead, transverse energy per unit rapidity ($\mathrm{d}E_{\mathrm{T}}/\mathrm{d}\eta$) is useful for such scaling between different collision energies shown in Fig. 3. $\overline{\mathrm{p}}/\pi^-$ ratio is scaled with this $\mathrm{d}E_{\mathrm{T}}/\mathrm{d}\eta$ value (($\mathrm{d}E_{\mathrm{T}}/\mathrm{d}\eta)^{1/3}$ used for comparison), but p/π^+ is not scaled. Proton yield at 62.4GeV is larger than that at 200GeV. This indicates that proton production at 62.4GeV is partly from baryon number transport, not only pair production.
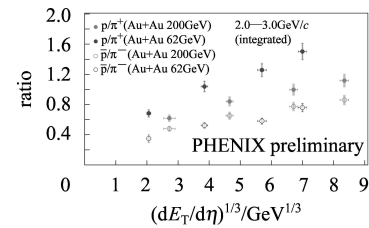

Fig. 3.   p/π ratio as a function of $(\mathrm{d}E_{\mathrm{T}}/\mathrm{d}\eta)^{1/3}$ for 2—3GeV/c in Au+Au at 62.4/200GeV.

3.2   Elliptic flow

In hydrodynamic models, elliptic flow, measured by the second Fourier coefficient v_2, can result from pressure gradient and initial spatial anisotropy of the collision overlap region. The spatial anisotropy is converted to momentum anisotropy by the pressure gradient, in other words, multiple scattering of particles. Eventually we observe the momentum anisotropy.

Figure 4(a) shows a comparison of $v_2(p_{\mathrm{T}})$ for identified particle species in minimum bias Au+Au collisions at $\sqrt{s_{\mathrm{NN}}} = 200$GeV. At low p_{T} (<1.5GeV/c),

a clear mass ordering is seen. But at higher p_T the mass ordering is broken, and v_2 seems to be dependent on the quark composition of the particles than on their mass. Fig. 4(b) shows the same v_2 plotted as a function of transverse kinetic energy KE_T ($=m_T-m$). In contrast to the mass ordering observed in Fig. 4(a), all particle species scale to a common curve at $KE_T < 1\text{GeV}/c$. For higher KE_T, this scaling gives a clear splitting into meson and baryon v_2's. Moreover, by scaling with the number of constituent quarks, we obtain a common v_2 curve for any particle types. This means that v_2 is developed in partonic level before hadrons form. This scaling feature supports the quark recombination picture for the hadron production[4].
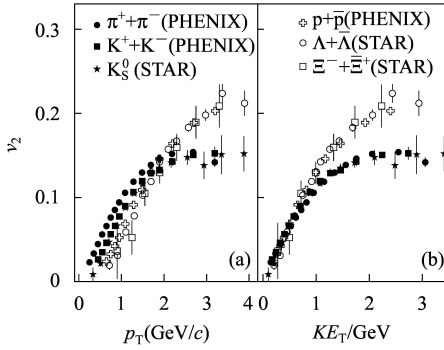

Fig. 4. v_2 vs. p_T (KE_T) for identified particle species in minimum bias Au+Au collisions at $\sqrt{s_{NN}} = 200\text{GeV}$[2].

Scaling of v_2 between different collision systems is tested. Fig. 5 shows v_2 as a function of N_{part} for different p_T for charged hadrons in Au+Au/Cu+Cu at $\sqrt{s_{NN}} = 200\text{GeV}$. v_2 does not look scaled by N_{part} in the overlapped region ($N_{part} \sim 80$). The initial spatial eccentricity should rather be an appropriate variable. The eccentricity is calculated by a Glauber model calculation, assuming the minor axis of the overlap region to be along the impact parameter vector. Actually v_2 looks scaled by this eccentricity shown in Fig. 6. It is also reported that v_2 is scaled by partici-
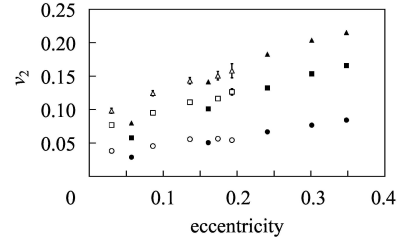
pant eccentricity, which accounts for nucleon position fluctuations in the colliding nuclei[6].
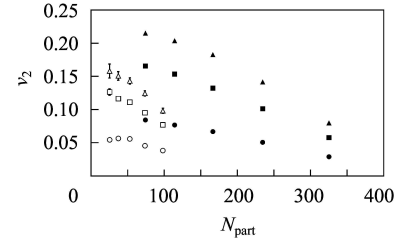
charged hadrons v_2
- Au+Au 200GeV, p_T=0.6GeV/c ○ Cu+Cu 200GeV, p_T=0.6GeV/c
- Au+Au 200GeV, p_T=1.4GeV/c □ Cu+Cu 200GeV, p_T=1.4GeV/c
▲ Au+Au 200GeV, p_T=2.3GeV/c ▵ Cu+Cu 200GeV, p_T=2.3GeV/c

Fig. 5. v_2 as a function of N_{part} for different p_T for charged hadrons in Au+Au/Cu+Cu at $\sqrt{s_{NN}} = 200\text{GeV}$.

charged hadrons v_2
- Au+Au 200GeV, p_T=0.6GeV/c ○ Cu+Cu 200GeV, p_T=0.6GeV/c
- Au+Au 200GeV, p_T=1.4GeV/c □ Cu+Cu 200GeV, p_T=1.4GeV/c
▲ Au+Au 200GeV, p_T=2.3GeV/c ▵ Cu+Cu 200GeV, p_T=2.3GeV/c

Fig. 6. v_2 as a function of eccentricity for different p_T for charged hadrons in Au+Au/Cu+Cu at $\sqrt{s_{NN}} = 200\text{GeV}$.

4 Summary

(Anti-)proton enhancement at intermediate p_T is confirmed in Au+Au/Cu+Cu collisions at $\sqrt{s_{NN}} = 62.4/200\text{GeV}$. We observe turnovers of p/π ratios at $p_T = 2$—$3\text{GeV}/c$, indicating a transition from soft to hard hadron production. The data sets show N_{part} scaling properties for p/π at same collision energies. While proton yield may be affected by baryon transport, $dE_T/d\eta$ scaling of $\overline{p}/\pi^-$ is also workable between different collision energies. Elliptic flow v_2 also shows several scaling properties such as quark number scaling, eccentricity scaling.

References

1 Adler S S et al. (PHENIX Collaboration). Phys. Rev., 2004, **C69**: 034910; Adler S S et al. (PHENIX Collaboration). Phys. Rev., 2004, **C69**: 034909; Adams J et al. (STAR Collaboration). Phys. Rev. Lett., 2004, **92**: 052302

2 Adare A et al. (PHENIX Collaboration). nucl-ex/0608033

3 Hirano T, Nara Y. Phys. Rev., 2004, **C69**: 034908

4 Fries R J, Muller B, Nonaka C et al. Phys. Rev., 2003, **C68**: 044902; Hwa R C, YANG C B. Phys. Rev., 2004, **C70**: 024905; Greco V, Ko C M, Levai P. Phys. Rev., 2003, **C68**: 034904

5 Abelev B I et al. (STAR Collaboration). Phys. Rev. Lett., 2006, **97**: 152301

6 Manly S et al. (PHOBOS Collaboration). Nucl. Phys., 2006, **A774**: 523